Experimental demonstration of a narrowband, angular tolerant, polarization independent, doubly periodic resonant grating filter

Anne-Laure Fehrembach,[1,*] Anne Talneau,[2] Olga Boyko,[2] Fabien Lemarchand,[1] and Anne Sentenac[1]

[1]*Institut Fresnel, CNRS UMR6133, Faculté de Saint Jérome (case 162), 13397 Marseille Cedex, France*
[2]*Laboratoire de Photonique et de Nanostructures, Route de Nozay, 91460 Marcoussis, France*
Corresponding author: anne-laure.fehrembach@fresnel.fr

Resonant grating filters are promising components for free-space narrowband filtering. Unfortunately, due to their weak angular tolerance, their performances are strongly deteriorated when they are illuminated with a standard collimated beam. Yet this problem can be overcome by resorting to a complex periodic pattern known as the doubly periodic grating [Lemarchand *et al.*, Opt. Lett. **23**, 1149 (1998)]. We report what we believe to be the first experimental fabrication and characterization of a bidimensional doubly periodic grating filter. We obtained a 0.5 nm bandpass polarization independent reflection filter for telecom wavelengths (1520–1570 nm) that presents a transmittivity minimum of 18% with a standard incident collimated beam. © 2007 Optical Society of America

OCIS codes: 050.2770, 120.2440, 230.4000, 310.2790, 260.5740.

Resonant grating filters are becoming increasingly attractive devices for narrowband filtering in free space. Composed of only a few waveguiding layers and a periodically textured interface, they permit one to reach experimentally a 0.1 nm bandpass [1]. The phenomenon underlying the resonant grating filter is the excitation, thanks to the periodic structuration, of a guided mode of the thin layers stack, which generates resonant peaks in the spectral reflectivity of the device. The peak linewidth decreases with the structuration strength (height and optical index contrast), which makes it convenient for narrowband filtering. Unfortunately, the angular tolerance of this resonance is very weak: The angular to spectral linewidth ratio is typically $0.5° \, \mathrm{nm}^{-1}$ under normal incidence and $0.1° \, \mathrm{nm}^{-1}$ under oblique incidence, whereas it is $17° \, \mathrm{nm}^{-1}$ for Fabry–Perot-based filters. The importance of this problem appears when one wants to use a narrowband (less than 1 nm) filter with a standard collimated beam (with a beam waist of 500 μm at 1550 nm). In this case, the divergence of the beam is usually larger than the angular tolerance of the filter. Thus, at the resonance wavelength, a part of the beam does not couple to the guided mode, leading to a loss of efficiency in the filtering process. Actually, most experimental demonstrations of narrow bandpass filtering by resonant gratings have been obtained with large beams [1–3] that are not usable in practical applications. Therefore, the crucial point is to enlarge the angular linewidth $\Delta\theta$ of the filter response while keeping a narrow spectral linewidth $\Delta\lambda$. This can be done with a careful optimization of the parameters of deep gratings [4,5] or by using a doubly periodic shallow grating [6,7]. In this Letter, we recall the basic principle of the doubly periodic grating. We extend it to gratings periodic along two directions (2D gratings), to design a polarization independent filter, and we demonstrate experimentally, for what we believe to be the first time, its interest and feasibility.

To identify the parameters of the structure governing the angular and spectral linewidths, some approximate theories have been developed for gratings periodic along one direction (1D). It has been proved [1,6] that when only one eigenmode is excited (e.g., in oblique incidence), both the angular and the spectral linewidths of the peak depend on the coupling strength between the incident field and the eigenmode. In the usual case where the eigenmode is excited through the first order of the grating, this coupling strength is related to the first Fourier harmonic of the grating permittivity, ϵ_1. When two counterpropagative modes are excited (e.g., in normal incidence, or in oblique incidence in special configurations [8]), the spectral linewidth still depends on the coupling strength between the incident field and the eigenmode (related to ϵ_1), while the angular linewidth depends on the coupling strength between the two modes, related to the second Fourier harmonic of the grating permittivity, ϵ_2. In the latter case, an independent tuning of the angular and spectral linewidths is possible. For lamellar gratings, composed of one single groove pattern [see inset in Fig. 1(a)], the ϵ_1 coefficient is always larger than the ϵ_2 coefficient, and the angular to spectral linewidths ratio stays below $0.5° \, \mathrm{nm}^{-1}$. To increase ϵ_2 with respect to ϵ_1, a complex basic pattern, composed with two grooves of different width [see inset in Fig. 1(b)], has been proposed [6]. In this case, the ϵ_2 coefficient can be much larger than ϵ_1, and a $\Delta\theta/\Delta\lambda$ ratio up to $7° \, \mathrm{nm}^{-1}$ has been numerically obtained. The benefit of such a pattern for narrowband filtering is illustrated in Fig. 1, where we plot the simulated transmittivity spectra of a basic lamellar grating and that of a doubly periodic grating illuminated with a Gaussian beam ($1/e^2$ diameter is 500 μm at the waist) under normal incidence. In our numerical code, the Gaussian beam is represented by its angular spectrum components [9], and the Fourier modal method [10] is used to calculate the transmittivity for each plane wave. Both
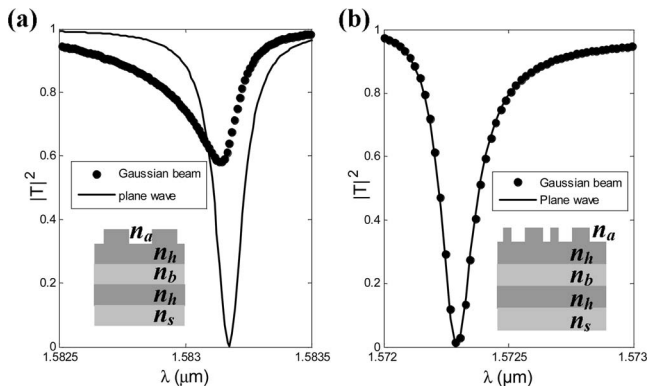
Fig. 1. Transmittivity spectra for (a) a single groove grating (period 971 nm, groove width 250 nm, height 13 nm, refractive index $n_a = 1$, $n_h = 2.07$, $n_b = 1.47$, and $n_s = 1.448$, and layer thickness, from top to bottom, 65, 113, and 196 nm). Fourier coefficients: $\epsilon_1 = 0.76$, $\epsilon_2 = 0.52$. (b) Doubly periodic grating (period 1047.5 nm, groove widths 241.25 and 281.25 nm, height 382.6 nm, refractive index $n_a = 1$, $n_h = 2.07$, $n_b = 1.47$, and $n_s = 1.448$, and layers thickness, from top to bottom, 62.5, 263.5, and 79.1 nm). Fourier coefficients: $\epsilon_1 = 0.09$, $\epsilon_2 = 1.04$.

structures have been designed to have a low sideband reflectance, a spectral linewidth of 0.1 nm, and a 100% filtering efficiency [11] when they are illuminated by a plane wave. Yet, when they are illuminated by a Gaussian beam, the filtering efficiency of the single groove grating falls dramatically, while it remains unchanged for the doubly periodic grating. In our opinion, this result is important since it forecasts the possibility to obtain experimentally nearly 100% narrowband filtering efficiency with standard collimators. Moreover, it can easily be extended to the oblique incidence configuration [8].

Another often requested property of filters is the polarization independence. The polarization independence requires the simultaneous excitation of two independent eigenmodes [12]. It is possible with a 2D grating illuminated under normal incidence. In this case, four counterpropagative eigenmodes are excited along the two directions of periodicity, and couple to each other by pairs [13], ensuring both polarization independence and angular tolerance. Note that the properties of this configuration can also be reproduced under oblique incidence [14]. The 2D doubly periodic grating pattern is composed of four circular holes, as depicted in Fig. 2(a), whose diameters have been designed to enhance the coupling between the counterpropagative modes as compared with the coupling of the incident beam to the modes. Its theoretical characteristics are $\Delta\theta = 0.17°$ and $\Delta\lambda = 0.24$ nm, when it is illuminated by a plane wave.

The component is composed of four layers (Ta_2O_5 and SiO_2) coated on a silica substrate using an electron-beam evaporation technique with a reactive ion beam assistance. Electron-beam lithography on a Leica EBPG 5000+ machine with a 2.5 nm grid using positive resist followed by a CHF3-based reactive ion etching process was performed on the top SiO_2 layer to define the doubly periodic lattice of holes. The component has been manufactured over a wide area
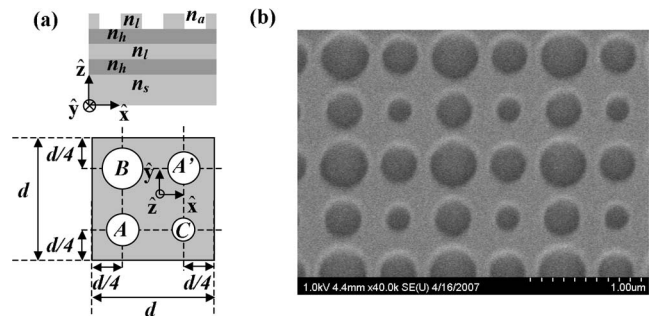

Fig. 2. Description of the manufactured component. (a) Top: four layers stack of Ta_2O_5 and SiO_2 on a glass substrate (refractive index $n_a = 1$, $n_h = 2.093$, $n_l = 1.47$, and $n_s = 1.443$, and layer thickness from top to bottom 220, 109, 63, and 126 nm, first is engraved). Bottom: periodic pattern (period $d = 960$ nm) of four air holes A, B, C, A' (diameters $d_a = 280$ nm, $d_b = 372.5$ nm, $d_c = 185$ nm, and $d_{a'} = d_a$). Fourier coefficients: $\epsilon_1 = 0.07$ and $\epsilon_2 = 0.17$. (b) Scanning electron microscopy image of the manufactured component.

(3 mm $\times 3$ mm) to minimize the finite size effects [4]. A scanning electron microscopy image of the manufactured component is shown in Fig. 2(b).

The resonant grating filter transmission has been measured using a tunable erbium fiber laser operating at a 1520–1570 nm range, with a 0.05 nm spectral linewidth. The light is coupled into a monomode fiber and then emitted through a telecom small fibered collimator. The resulting beam light presents a Gaussian profile. The grating is placed at the waist of the beam ($1/e^2$ diameter$=580$ μm). Collimator–grating distance and collimator–detector distance (f and $2f$, respectively) are chosen to provide a configuration analog to a fiber–fiber mounting. Transmission of the resonant grating is evaluated by comparing the signal with and without grating.

The transmission spectra for normal incidence are represented in Fig. 3(a) for $\hat{s}$ polarization (squares) and $\hat{p}$ polarization (stars), while the experimental results were obtained with an intermediate incident polarization (circles). We observe that the transmittivity minima obtained experimentally and theoretically with the Gaussian beam are similar. Hence, the
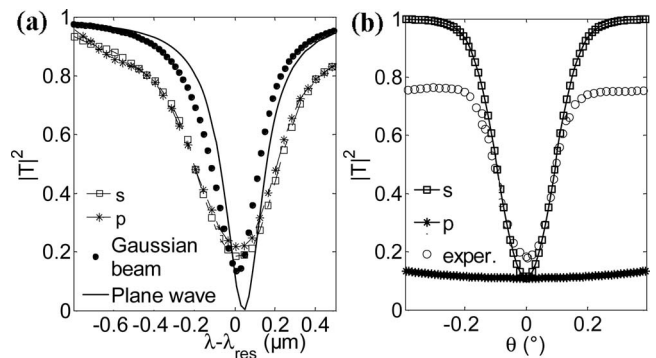

Fig. 3. (a) Transmittivity spectra for the component of Fig. 2: experimentally (squares and stars, $\lambda_{res} = 1.53286$ μm) and theoretically (dots and solid curve, $\lambda_{res} = 1.55181$ μm). (b) Transmittivity with respect to the angle of incidence: experimentally for an intermediate polarization (circles) and theoretically (squares and stars). Gaussian beam $1/e^2$ diameter $= 580$ μm.

loss of filtering efficiency is mainly due to the weak angular tolerance of the peak (0.17°) as compared with the beam divergence (0.2°). On the other hand, the linewidth broadening is essentially imputed to etching imperfections, which break the pattern periodicity and generate diffusion. The transmission with respect to the incidence angle θ [with respect to the (Oz) axis, in the (Oxz) plane] is plotted in Fig. 3(b). The large angular tolerance obtained in $\hat{\mathbf{p}}$ polarization as compared with $\hat{\mathbf{s}}$ polarization is easily explained by considering the coupling condition of the guided mode. For an incidence wave vector in the (Oxz) plane, with a wavelength λ and an incidence angle θ, the resonance peak occurs if

$$\left| \frac{2\pi}{\lambda} \sin \theta \, \hat{\mathbf{x}} \pm \mathbf{K} \right| = k_g, \tag{1}$$

where $\mathbf{K}$ is a vector of the reciprocal lattice of the periodic structure and k_g represents the propagation constant of the excited eigenmode. For $\hat{\mathbf{s}}$ polarization (electric field along $\hat{\mathbf{y}}$), and for a TE guided mode (which is the case for the studied configuration), the incident field couples to the guided mode through the reciprocal lattice vector $\mathbf{K}=2\pi/d\,\hat{\mathbf{x}}$. On the contrary, for $\hat{\mathbf{p}}$ polarization (magnetic field along $\hat{\mathbf{y}}$), the incident field couples to the TE guided mode through $\mathbf{K}$ $=2\pi/d\,\hat{\mathbf{y}}$. Obviously, the coupling condition in Eq. (1) is more robust with respect to the incidence angle in the latter case than in the former. This explains the angular responses obtained theoretically for $\hat{\mathbf{s}}$ and $\hat{\mathbf{p}}$ polarization, and the experimental curve obtained for an intermediate polarization, which is a linear combination of the $\hat{\mathbf{s}}$ and $\hat{\mathbf{p}}$ cases.

Last, we study the transmittivity versus the incidence angle and wavelength (Fig. 4). On this pseudo-dispersion relation, one can see the usual band edges obtained with resonant gratings [15] and an extra straight line, that is tangential to the lower band edge (for $\theta=0$ and λ close to 1.545 μm). This feature is a result of the experimental incidence linear polarization possessing an $\hat{\mathbf{s}}$ and a $\hat{\mathbf{p}}$ component. The $\hat{\mathbf{s}}$

component excites two counterpropagative modes in the (Ox) direction, and generates the lower and higher band edges, while the $\hat{\mathbf{p}}$ component excites two counterpropagative modes in the (Oy) direction, and generates the angular tolerant resonance, as explained in the previous paragraph. Finally, note that the higher band edge disappears about normal incidence. This corresponds to a mode whose field is antisymmetrical with respect to the (Oyz) plane, and thus which cannot be excited with an incident beam under normal incidence.

As a conclusion, we have shown that obtaining a 0.1 nm bandpass filter with 100% filtering efficiency is possible with the doubly periodic grating while it is impossible with a single groove grating, when the component is illuminated with a standard Gaussian beam (diameter 500 μm at the waist for a 1550 nm wavelength). We demonstrated the feasibility of 2D doubly periodic gratings and their interest for unpolarized narrowband filtering by obtaining experimentally a 0.5 nm bandpass polarization independent reflection filter at telecom wavelength (1520–1570 nm), with a transmittivity minimum of 18%, under normal incidence, with a standard collimated beam. We believe that this encouraging experimental result paves the way for the use of resonant grating filters in standard fiber–fiber mountings. Our work is now oriented to the fabrication of an angular tolerant doubly periodic grating filter functionning under oblique incidence [14] and to the improvement of the manufacturing process to fabricate components closer to the designed ones.

References

1. D. Rosenblatt, A. Sharon, and A. A. Friesem, IEEE J. Quantum Electron. **33**, 2038 (1997).
2. D. W. Peters, S. A. Kemme, and G. R. Hadley, J. Opt. Soc. Am. A **21**, 981 (2004).
3. G. Niederer, H. P. Herzig, J. Shamir, H. Thiele, M. Schnieper, and C. Zschokke, Appl. Opt. **43**, 1683 (2004).
4. J. M. Bendickson, E. N. Glytsis, T. G. Gaylord, and D. L. Brundett, J. Opt. Soc. Am. A **18**, 1912 (2001).
5. D. K. Jacob, S. C. Dunn, and M. G. Moharam, J. Opt. Soc. Am. A **18**, 2109 (2001).
6. F. Lemarchand, A. Sentenac, and H. Giovannini, Opt. Lett. **23**, 1149 (1998).
7. A. Mizutani, H. Kikuta, and K. Iwata, Opt. Rev. **10**, 13 (2003).
8. A. Sentenac and A.-L. Fehrembach, J. Opt. Soc. Am. A **22**, 475 (2005).
9. P. C. Chaumet, J. Opt. Soc. Am. A **23**, 3197 (2005).
10. L. Li, J. Opt. Soc. Am. A **14**, 2758 (1997).
11. E. Popov, L. Mashev, and D. Maystre, Opt. Acta **33**, 607 (1986).
12. A.-L. Fehrembach, D. Maystre, and A. Sentenac, J. Opt. Soc. Am. A **19**, 1136 (2002).
13. A.-L. Fehrembach and A. Sentenac, J. Opt. Soc. Am. A **20**, 481 (2003).
14. A.-L. Fehrembach and A. Sentenac, Appl. Phys. Lett. **86**, 121105 (2005).
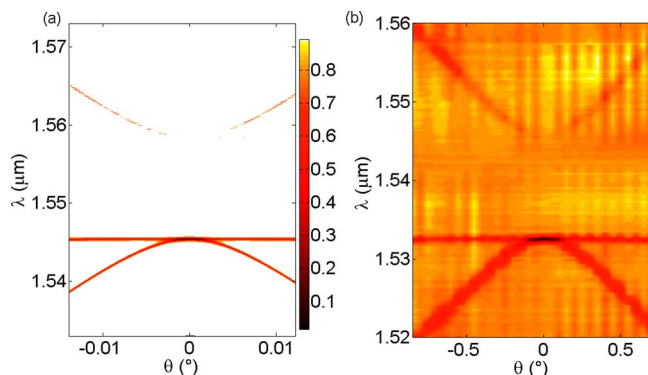15. W. Barnes, T. Preist, S. Kitson, and J. R. Sambles, Phys. Rev. B **54**, 6227 (1996).

Fig. 4.   (Color online) Transmittivity with respect to the angle and wavelength of incidence for the component of Fig. 2. (a) Theoretically (polarization median between *s* and *p*) and (b) experimentally (intermediate polarization).